

Measurement of the branching fraction ratio

$$\mathcal{B}(B_c^+ \rightarrow \psi(2S)\pi^+)/\mathcal{B}(B_c^+ \rightarrow J/\psi\pi^+)$$

R. Aaij *et al.*^{*}

(LHCb collaboration)

(Received 14 July 2015; published 20 October 2015)

Using pp collision data collected by LHCb at center-of-mass energies $\sqrt{s} = 7$ TeV and 8 TeV, corresponding to an integrated luminosity of 3 fb^{-1} , the ratio of the branching fraction of the $B_c^+ \rightarrow \psi(2S)\pi^+$ decay relative to that of the $B_c^+ \rightarrow J/\psi\pi^+$ decay is measured to be $0.268 \pm 0.032(\text{stat}) \pm 0.007(\text{syst}) \pm 0.006(\text{BF})$. The first uncertainty is statistical, the second is systematic, and the third is due to the uncertainties on the branching fractions of the $J/\psi \rightarrow \mu^+\mu^-$ and $\psi(2S) \rightarrow \mu^+\mu^-$ decays. This measurement is consistent with the previous LHCb result, and the statistical uncertainty is halved.

DOI: 10.1103/PhysRevD.92.072007

PACS numbers: 13.25.Hw, 14.40.Nd, 12.38.Qk

In the Standard Model of particle physics the B_c meson family is unique because it contains two different heavy flavor quarks, charm and beauty. The ground state of the B_c meson family has a rich set of decay modes since either constituent quark can decay with the other as a spectator, or they can annihilate to a virtual W boson. The search for new B_c^+ decay channels¹ and precise measurements of their branching fractions can improve the understanding of quantum chromodynamics (QCD) and can test various effective models. Many properties of the B_c^+ meson have been investigated by the LHCb experiment: the B_c^+ mass, lifetime and production rate have been measured [1–6], while several new decay channels have been observed [2,3,7–13]. The observation of the $B_c^+ \rightarrow \psi(2S)\pi^+$ decay was made with pp collision data at a center-of-mass energy of $\sqrt{s} = 7$ TeV, corresponding to an integrated luminosity of 1.0 fb^{-1} [8]. The ratio of the branching fraction of the $B_c^+ \rightarrow \psi(2S)\pi^+$ decay with respect to that of the $B_c^+ \rightarrow J/\psi\pi^+$ decay, defined as

$$R_B \equiv \frac{\mathcal{B}(B_c^+ \rightarrow \psi(2S)\pi^+)}{\mathcal{B}(B_c^+ \rightarrow J/\psi\pi^+)}, \quad (1)$$

was measured to be $0.250 \pm 0.068(\text{stat}) \pm 0.014(\text{syst}) \pm 0.006(\text{BF})$. The first uncertainty is statistical, the second is systematic, and the third is due to the uncertainties on the branching fractions of the $J/\psi \rightarrow \mu^+\mu^-$ and $\psi(2S) \rightarrow \mu^+\mu^-$ decays. The statistical uncertainty is dominant. Several theoretical predictions for R_B based on different effective models [14–19] exist, and vary between 0.07 and 0.29.

^{*}Full author list given at end of the article.

Published by the American Physical Society under the terms of the [Creative Commons Attribution 3.0 License](#). Further distribution of this work must maintain attribution to the author(s) and the published article's title, journal citation, and DOI.

¹Charge conjugation is implied throughout the paper.

The analysis presented here updates the previous LHCb measurement of R_B [8], using the full pp collision data collected by LHCb in 2011 and 2012 at $\sqrt{s} = 7$ TeV and 8 TeV, respectively, corresponding to an integrated luminosity of 3 fb^{-1} . Due to the increased data sample and an improved analysis method, the statistical uncertainty is reduced by half, allowing a more powerful test of the theories.

The LHCb detector [20,21] is a single-arm forward spectrometer covering the pseudorapidity range $2 < \eta < 5$, and is designed for the study of particles containing b or c quarks. The detector includes a high-precision tracking system consisting of a silicon-strip vertex detector surrounding the pp interaction region [22], a large-area silicon-strip detector located upstream of a dipole magnet with a bending power of about 4 Tm, and three stations of silicon-strip detectors and straw drift tubes [23] placed downstream of the magnet. The tracking system provides a measurement of momentum, p , of charged particles with a relative uncertainty that varies from 0.5% at low momentum to 1.0% at 200 GeV/ c . The minimum distance of a track to a primary vertex (PV), the impact parameter, is measured with a resolution of $(15 + 29/p_T)\mu\text{m}$, where p_T is the component of the track momentum transverse to the beam, in GeV/ c . Different types of charged hadrons are distinguished using information from two ring-imaging Cherenkov detectors [24]. Photons, electrons, and hadrons are identified by a calorimeter system consisting of scintillating-pad and preshower detectors, an electromagnetic calorimeter, and a hadronic calorimeter. Muons are identified by a system composed of alternating layers of iron and multiwire proportional chambers [25]. The online event selection is performed by a trigger [26], which consists of a hardware stage, based on information from the calorimeter and muon systems, followed by a software stage, which applies a full event reconstruction.

In the $B_c^+ \rightarrow J/\psi\pi^+$ and $B_c^+ \rightarrow \psi(2S)\pi^+$ decay channels, the J/ψ and $\psi(2S)$ mesons are reconstructed through their decays into two muons. At least one muon with high

p_T is required in the hardware trigger. The software trigger requires a charged particle with $p_T > 1.7 \text{ GeV}/c$, or $p_T > 1 \text{ GeV}/c$ if identified as a muon; alternatively a dimuon trigger requires two oppositely charged muons with $p_T > 500 \text{ MeV}/c$, and the invariant mass of the muon pair greater than $2.95 \text{ GeV}/c^2$.

Further offline selections require a good quality muon track with $p_T > 550 \text{ MeV}/c$, a good quality vertex for the reconstructed J/ψ or $\psi(2S)$ candidate, and the reconstructed J/ψ and $\psi(2S)$ masses to be within $\pm 100 \text{ MeV}/c^2$ of their known values [27]. The mass resolution for both resonances is $14 \text{ MeV}/c^2$. The muon track pair and the pion track are required to be inconsistent with originating from a PV. The pion track is required to be of good quality, and to have a p_T greater than $500 \text{ MeV}/c$. The particle identification (PID) information for pions is used to reduce the contamination from kaons and protons. The B_c^+ candidate is required to have a good quality vertex and a reconstructed mass within $\pm 500 \text{ MeV}/c^2$ of its known mass [27], which corresponds to more than ten times the mass resolution. To further separate signal from background, a boosted decision tree (BDT) selection using the AdaBoost algorithm [28,29] is applied. The selection uses more input variables and is more sophisticated compared to the previous analysis [8].

Simulated samples are generated to study the behavior of signal events. The B_c^+ signals are generated with a dedicated generator BCVEGPY [30,31] through the dominant hard subprocess $gg \rightarrow B_c^+ + b + \bar{c}$. The fragmentation and hadronization processes are simulated with PYTHIA [32,33]. The detector simulation is based on the GEANT4 package [34,35]. The BDT classifier uses information on the candidate's kinematic properties, decay length, vertex quality, impact parameter, and angle between the particle momentum and the vector from the primary to the secondary vertex. The distributions of the variables that are used in the BDT are similar for $B_c^+ \rightarrow J/\psi\pi^+$ and $B_c^+ \rightarrow \psi(2S)\pi^+$ decays. The simulated sample of $B_c^+ \rightarrow J/\psi\pi^+$ is used as the signal sample for the BDT training. The main background is combinatorial, and is represented by the upper sideband in the B_c^+ mass spectrum from the $B_c^+ \rightarrow J/\psi\pi^+$ data sample, requiring the reconstructed mass to be in the range $[6346, 6444] \text{ MeV}/c^2$. Since the upper sideband is used for the BDT training, the BDT could overperform in this region and distort the expected combinatorial background in the signal region. To avoid possible bias, two BDT classifiers are trained, denoted as BDT1 and BDT2 in the following. The $B_c^+ \rightarrow J/\psi\pi^+$ simulation and data samples are both split into two halves. One half of the simulated data sample and of the B_c^+ upper

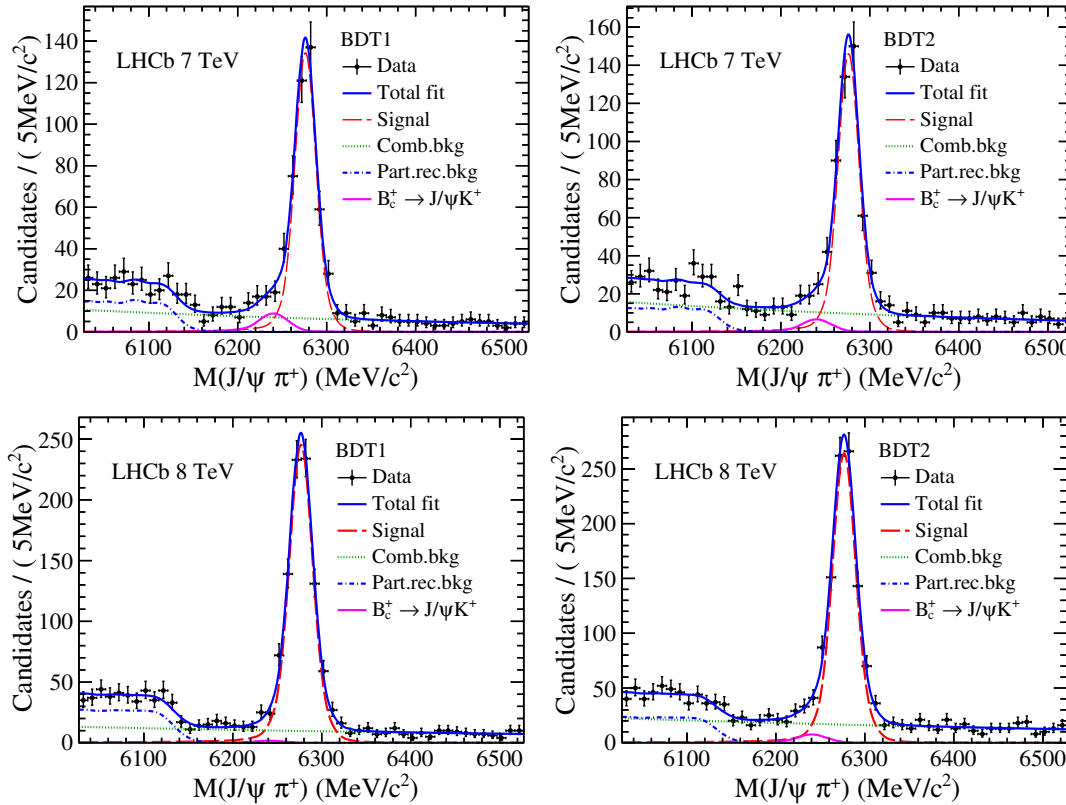


FIG. 1 (color online). Fit to the reconstructed B_c^+ mass distribution for $B_c^+ \rightarrow J/\psi\pi^+$ using (top) 2011 and (bottom) 2012 data samples. The plots on the left (right) correspond to the data selected with BDT1 (BDT2). Black points with error bars represent the data, and the various components are indicated in the keys.

sideband is used to train the BDT1 classifier, and the other half for BDT2. Each BDT classifier is applied to the other half of the $B_c^+ \rightarrow J/\psi\pi^+$ data sample, which is not used for its training. The $B_c^+ \rightarrow \psi(2S)\pi^+$ data sample is also split into two subsamples, one for each BDT classifier. The threshold value for the BDT response is chosen to maximize the signal significance. Finally, the $\mu^+\mu^-$ invariant mass window [3030, 3170] MeV/ c^2 is applied to J/ψ candidates, and [3620, 3760] MeV/ c^2 to $\psi(2S)$ candidates.

After the full selection, the background in the $B_c^+ \rightarrow J/\psi\pi^+$ sample consists of three categories: combinatorial background; partially reconstructed background, mainly from $B_c^+ \rightarrow J/\psi\rho^+$ decays with $\rho^+ \rightarrow \pi^+\pi^0$, where the π^0 is not reconstructed; and contamination from the Cabibbo-suppressed decay, $B_c^+ \rightarrow J/\psi K^+$, with the kaon misidentified as a pion. The background in the $B_c^+ \rightarrow \psi(2S)\pi^+$ sample consists of a combinatorial background and a partially reconstructed background. The contribution from $B_c^+ \rightarrow \psi(2S)K^+$ is negligible.

The signal yields are extracted from unbinned extended maximum likelihood fits to the invariant mass distributions of $J/\psi\pi^+$ or $\psi(2S)\pi^+$ in the range [6027, 6527] MeV/ c^2 , as shown in Figs. 1 and 2 for 2011 and 2012 data, and are summarized in Tables I and II. To improve the B_c^+ mass resolution, the masses of J/ψ and $\psi(2S)$ candidates are

constrained to their known values [27]. For the $B_c^+ \rightarrow J/\psi\pi^+$ channel, the signal probability density function is modeled by the sum of two double-sided Crystal Ball functions [36], with the same mean value and tail parameters determined from simulation; the combinatorial background is described with an exponential function; and the partially reconstructed background is modeled with the distribution of the B_c^+ invariant mass obtained from a simulated $B_c^+ \rightarrow J/\psi\rho^+$ sample using a kernel estimation [37]. This last shape is convolved with a Gaussian distribution to take into account a difference in mass resolution between data and simulation. For the $B_c^+ \rightarrow J/\psi K^+$ background, the shape of the B_c^+ mass distribution is modeled by a double-sided Crystal Ball function with parameters determined from simulation. For the $B_c^+ \rightarrow \psi(2S)\pi^+$ channel, due to the limited statistics, the signal shape is modeled by a single double-sided Crystal Ball function with the tail parameters determined from simulation; the combinatorial and partially reconstructed backgrounds are described with the same models as used for the $B_c^+ \rightarrow J/\psi\pi^+$ channel.

The total selection efficiency is the product of the detector geometrical acceptance, the trigger efficiency, the reconstruction and selection efficiency, the PID efficiency, and the BDT classifier efficiency. All efficiencies are determined using simulated samples. To account for any

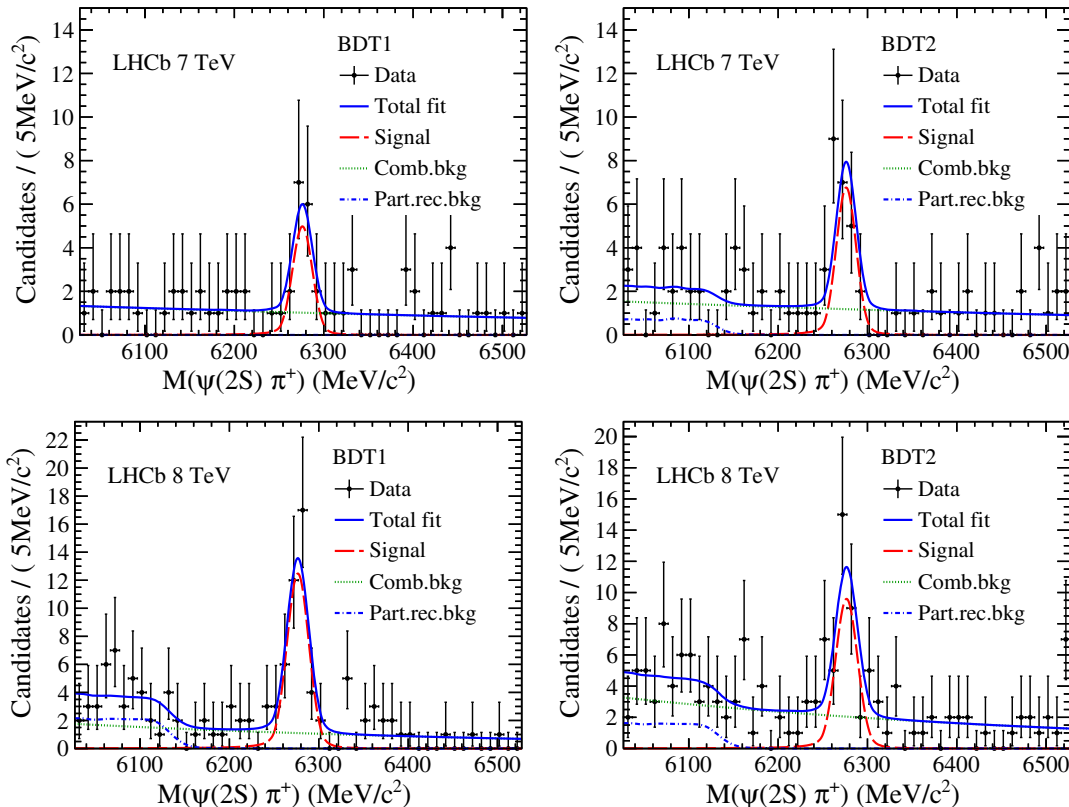


FIG. 2 (color online). Fit to the reconstructed B_c^+ mass distribution for $B_c^+ \rightarrow \psi(2S)\pi^+$ using (top) 2011 and (bottom) 2012 data samples. The plots on the left (right) correspond to the data selected with BDT1 (BDT2). Black points with error bars represent the data, and the various components are indicated in the keys.

TABLE I. Summary of the signal yields and efficiencies for the $B_c^+ \rightarrow J/\psi\pi^+$ decay.

	2011		2012	
	BDT1	BDT2	BDT1	BDT2
Yield	437 ± 24	475 ± 26	883 ± 34	950 ± 36
ε_{BDT}	$(62.99 \pm 0.07)\%$	$(69.29 \pm 0.06)\%$	$(62.33 \pm 0.06)\%$	$(68.50 \pm 0.06)\%$
ε^*	$(1.392 \pm 0.003)\%$		$(1.339 \pm 0.003)\%$	

discrepancy between data and simulation, the PID efficiencies are calibrated using a π^+ sample from D^* -tagged $D^0 \rightarrow K^-\pi^+$ decays. The BDT classifier efficiencies of BDT1 and BDT2 are slightly different. After correcting for the BDT classifier efficiencies the signal yields of the subsamples are consistent within the statistical uncertainties. The BDT classifier efficiency, ε_{BDT} , and the product of all other efficiencies, ε^* , are listed in Tables I and II.

Several sources of systematic uncertainty on the R_B measurement are studied and are summarized in Table III. To account for the uncertainty due to the signal shape modeling, the data are refitted with an alternative shape. The B_c^+ invariant mass distributions are modeled by a kernel estimation convolved with a Gaussian function, as determined from simulation. A difference of 0.6% from the nominal result is observed and is taken as a systematic uncertainty.

The modeling of the partially reconstructed background can also introduce a systematic uncertainty. This is estimated by reducing the fit range to [6164, 6527] MeV/ c^2 to exclude its contribution. A change of 2.4% in the result is observed. In the nominal fits, the parameters for $B_c^+ \rightarrow J/\psi K^+$ and the partially reconstructed background are fixed; the results change by less than 1% when these parameters are allowed to vary. The systematic uncertainty due to background modeling is estimated to be 2.4%.

Systematic uncertainties on the R_B measurement can be introduced by the BDT classifier efficiency if the simulation fails to describe the data. The distributions of all training variables from simulation and background-subtracted data are compared, where the background subtraction is performed using the *sPlot* technique, taking the B_c^+ invariant mass as the discriminating variable [38]. They are generally in agreement within statistical fluctuations. Only one variable, which describes the consistency between the pion track and the PV, indicates small differences between simulation and data. Therefore, the

simulated sample is reweighed to match the data, and the BDT efficiencies are recalculated with the reweighed simulated sample. The result obtained with these BDT efficiencies is different from the nominal value by 0.2%, which is taken as the uncertainty from the BDT classifier.

The efficiencies determined from simulated samples have uncertainties due to the limited statistics. This leads to an uncertainty of 0.3%. An uncertainty of 1.1% is assigned due to imperfect simulation of the trigger, which is determined using data driven methods [39,40]. The B_c^+ lifetime of simulated samples is set according to the latest LHCb measurement [4]. To estimate the systematic uncertainty due to this, the B_c^+ lifetime is varied within the uncertainty of this measurement, and the change in the result, 0.1%, is taken as a systematic uncertainty. The total systematic uncertainty is 2.7%.

The ratio of the branching fractions with J/ψ and $\psi(2S)$ mesons decaying to dimuons, denoted as

$$R \equiv \frac{\mathcal{B}(B_c^+ \rightarrow \psi(2S)\pi^+, \psi(2S) \rightarrow \mu^+\mu^-)}{\mathcal{B}(B_c^+ \rightarrow J/\psi\pi^+, J/\psi \rightarrow \mu^+\mu^-)}, \quad (2)$$

is calculated as

$$R = \frac{N_{2011}^{\text{cor}}(B_c^+ \rightarrow \psi(2S)\pi^+) + N_{2012}^{\text{cor}}(B_c^+ \rightarrow \psi(2S)\pi^+)}{N_{2011}^{\text{cor}}(B_c^+ \rightarrow J/\psi\pi^+) + N_{2012}^{\text{cor}}(B_c^+ \rightarrow J/\psi\pi^+)}, \quad (3)$$

where $N_{2011(2012)}^{\text{cor}}$ are the signal yields from 2011 (2012) after efficiency correction. The ratio is measured to be

$$R = 0.0354 \pm 0.0042(\text{stat}) \pm 0.0010(\text{syst}).$$

The ratio of the branching fractions of $B_c^+ \rightarrow \psi(2S)\pi^+$ and $B_c^+ \rightarrow J/\psi\pi^+$ is calculated as

TABLE II. Summary of the signal yields and efficiencies for the $B_c^+ \rightarrow \psi(2S)\pi^+$ decay.

	2011		2012	
	BDT1	BDT2	BDT1	BDT2
Yield	14.4 ± 4.5	19.6 ± 5.3	40.1 ± 7.1	30.8 ± 7.0
ε_{BDT}	$(58.79 \pm 0.11)\%$	$(65.84 \pm 0.11)\%$	$(58.32 \pm 0.08)\%$	$(65.08 \pm 0.08)\%$
ε^*	$(1.631 \pm 0.006)\%$		$(1.529 \pm 0.005)\%$	

TABLE III. Summary of systematic uncertainties on the R_B measurement.

Component	Uncertainty
Signal shape	0.6%
Background shape	2.4%
BDT classifier	0.2%
Monte-Carlo statistics	0.3%
Trigger efficiency	1.1%
B_c^+ lifetime	0.1%
Total	2.7%

$$R_B = R \times \frac{\mathcal{B}(J/\psi \rightarrow \mu^+ \mu^-)}{\mathcal{B}(\psi(2S) \rightarrow \mu^+ \mu^-)}. \quad (4)$$

Assuming electroweak universality, the $J/\psi \rightarrow \mu^+ \mu^-$ and $\psi(2S) \rightarrow \mu^+ \mu^-$ branching fractions can be substituted with the more precisely measured ones in the $e^+ e^-$ channel [27]. Using these values, the ratio R_B is measured to be

$$R_B = 0.268 \pm 0.032(\text{stat}) \pm 0.007(\text{syst}) \pm 0.006(\text{BF}),$$

where the first uncertainty is statistical, the second is systematic, and the last term is due to the uncertainty on $\mathcal{B}(J/\psi \rightarrow e^+ e^-)/\mathcal{B}(\psi(2S) \rightarrow e^+ e^-)$. This result is in agreement with the previous LHCb result [8]. Our measurement is consistent with the predictions of nonrelativistic QCD at next-to-leading order ($0.26^{+0.05}_{-0.06}$) [18] and perturbative QCD based on k_T factorization ($0.29^{+0.17}_{-0.11}$) [19]. The result disfavors the theoretical calculations based on the relativistic quark model [14], the quark potential model

[15], the relativistic constituent quark model [16], and the QCD relativistic potential model [17].

ACKNOWLEDGMENTS

We express our gratitude to our colleagues in the CERN accelerator departments for the excellent performance of the LHC. We thank the technical and administrative staff at the LHCb institutes. We acknowledge support from CERN and from the national agencies: CAPES, CNPq, FAPERJ and FINEP (Brazil); NSFC (China); CNRS/IN2P3 (France); BMBF, DFG, HGF and MPG (Germany); INFN (Italy); FOM and NWO (The Netherlands); MNiSW and NCN (Poland); MEN/IFA (Romania); MinES and FANO (Russia); MinECo (Spain); SNSF and SER (Switzerland); NASU (Ukraine); STFC (United Kingdom); NSF (USA). The Tier1 computing centres are supported by IN2P3 (France), KIT and BMBF (Germany), INFN (Italy), NWO and SURF (The Netherlands), PIC (Spain), GridPP (United Kingdom). We are indebted to the communities behind the multiple open source software packages on which we depend. We are also thankful for the computing resources and the access to software R&D tools provided by Yandex LLC (Russia). Individual groups or members have received support from EPLANET, Marie Skłodowska-Curie Actions and ERC (European Union), Conseil général de Haute-Savoie, Labex ENIGMASS and OCEVU, Région Auvergne (France), RFBR (Russia), XuntaGal and GENCAT (Spain), Royal Society and Royal Commission for the Exhibition of 1851 (United Kingdom).

-
- [1] R. Aaij *et al.* (LHCb Collaboration), Measurements of B_c^+ production and mass with the $B_c^+ \rightarrow J/\psi \pi^+$ decay, *Phys. Rev. Lett.* **109**, 232001 (2012).
 - [2] R. Aaij *et al.* (LHCb Collaboration), Observation of $B_c^+ \rightarrow J/\psi D_s^+$ and $B_c^+ \rightarrow J/\psi D_s^{*+}$ decays, *Phys. Rev. D* **87**, 112012 (2013).
 - [3] R. Aaij *et al.* (LHCb Collaboration), First observation of a baryonic B_c^+ decay, *Phys. Rev. Lett.* **113**, 152003 (2014).
 - [4] R. Aaij *et al.* (LHCb Collaboration), Measurement of the B_c^+ meson lifetime using $B_c^+ \rightarrow J/\psi \mu^+ \nu_\mu X$ decays, *Eur. Phys. J. C* **74**, 2839 (2014).
 - [5] R. Aaij *et al.* (LHCb Collaboration), Measurement of the lifetime of the B_c^+ meson using the $B_c^+ \rightarrow J/\psi \pi^+$ decay mode, *Phys. Lett. B* **742**, 29 (2015).
 - [6] R. Aaij *et al.* (LHCb Collaboration), Measurement of B_c^+ production in proton-proton collisions at $\sqrt{s} = 8$ TeV, *Phys. Rev. Lett.* **114**, 132001 (2015).
 - [7] R. Aaij *et al.* (LHCb Collaboration), First observation of the decay $B_c^+ \rightarrow J/\psi \pi^+ \pi^- \pi^+$, *Phys. Rev. Lett.* **108**, 251802 (2012).
 - [8] R. Aaij *et al.* (LHCb Collaboration), Observation of the decay $B_c^+ \rightarrow \psi(2S) \pi^+$, *Phys. Rev. D* **87**, 071103(R) (2013).
 - [9] R. Aaij *et al.* (LHCb Collaboration), First observation of the decay $B_c^+ \rightarrow J/\psi K^+$, *J. High Energy Phys.* **09** (2013) 075.
 - [10] R. Aaij *et al.* (LHCb Collaboration), observation of the decay $B_c^+ \rightarrow B_s^0 \pi^+$, *Phys. Rev. Lett.* **111**, 181801 (2013).
 - [11] R. Aaij *et al.* (LHCb Collaboration), Observation of the decay $B_c^+ \rightarrow J/\psi K^+ K^- \pi^+$, *J. High Energy Phys.* **11** (2013) 094.
 - [12] R. Aaij *et al.* (LHCb Collaboration), Evidence for the decay $B_c^+ \rightarrow J/\psi 3\pi^+ 2\pi^-$, *J. High Energy Phys.* **05** (2014) 148.
 - [13] R. Aaij *et al.* (LHCb Collaboration), Measurement of the ratio of B_c^+ branching fractions to $J/\psi \pi^+$ and $J/\psi \mu^+ \nu_\mu$ final states, *Phys. Rev. D* **90**, 032009 (2014).
 - [14] D. Ebert, R. N. Faustov, and V. O. Galkin, Weak decays of the B_c meson to charmonium and D mesons in the relativistic quark model, *Phys. Rev. D* **68**, 094020 (2003).
 - [15] C.-H. Chang and Y.-Q. Chen, Decays of the B_c meson, *Phys. Rev. D* **49**, 3399 (1994).

- [16] J.-F. Liu and K.-T. Chao, B_c meson weak decays and CP violation, *Phys. Rev. D* **56**, 4133 (1997).
- [17] P. Colangelo and F. De Fazio, Using heavy quark spin symmetry in semileptonic B_c decays, *Phys. Rev. D* **61**, 034012 (2000).
- [18] C.-F. Qiao, P. Sun, D. Yang, and R.-L. Zhu, B_c exclusive decays to charmonium and a light meson at next-to-leading order accuracy, *Phys. Rev. D* **89**, 034008 (2014).
- [19] Z. Rui, W.-Fei Wang, G.-Xin Wang, Li-Hua Song, and C.-Dian Lü, The $B_c \rightarrow \psi(2S)\pi$, $\eta_c(2S)\pi$ decays in the perturbative QCD approach, *Eur. Phys. J. C* **75**, 293 (2015).
- [20] A. A. Alves Jr. *et al.* (LHCb Collaboration), The LHCb detector at the LHC, *J. Instrum.* **3**, S08005 (2008).
- [21] R. Aaij *et al.* (LHCb Collaboration), LHCb detector performance, *Int. J. Mod. Phys. A* **30**, 1530022 (2015).
- [22] R. Aaij *et al.*, Performance of the LHCb vertex locator, *J. Instrum.* **9**, P09007 (2014).
- [23] R. Arink *et al.*, Performance of the LHCb outer tracker, *J. Instrum.* **9**, P01002 (2014).
- [24] M. Adinolfi *et al.*, Performance of the LHCb RICH detector at the LHC, *Eur. Phys. J. C* **73**, 2431 (2013).
- [25] A. A. Alves Jr. *et al.*, Performance of the LHCb muon system, *J. Instrum.* **8**, P02022 (2013).
- [26] R. Aaij *et al.*, The LHCb trigger and its performance in 2011, *J. Instrum.* **8**, P04022 (2013).
- [27] K. A. Olive *et al.* (Particle Data Group), Review of particle physics, *Chin. Phys. C* **38**, 090001 (2014).
- [28] L. Breiman, J. H. Friedman, R. A. Olshen, and C. J. Stone, *Classification and Regression Trees* (Wadsworth International Group, Belmont, CA, 1984).
- [29] R. E. Schapire and Y. Freund, A decision-theoretic generalization of on-line learning and an application to boosting, *J. Comput. Syst. Sci.* **55**, 119 (1997).
- [30] C.-H. Chang, C. Driouichi, P. Eerola, and X. G. Wu, BCVEGPY: An event generator for hadronic production of the B_c meson, *Comput. Phys. Commun.* **159**, 192 (2004).
- [31] C.-H. Chang, J.-X. Wang, and X.-G. Wu, BCVEGPY2.0: An upgraded version of the generator BCVEGPY with the addition of hadroproduction of the P-wave B_c states, *Comput. Phys. Commun.* **174**, 241 (2006).
- [32] T. Sjöstrand, S. Mrenna, and P. Skands, PYTHIA 6.4 physics and manual, *J. High Energy Phys.* **05** (2006) 026.
- [33] I. Belyaev *et al.*, Handling of the generation of primary events in Gauss, the LHCb simulation framework, *J. Phys. Conf. Ser.* **331**, 032047 (2011).
- [34] S. Agostinelli *et al.* (Geant4 Collaboration), Geant4: A simulation toolkit, *Nucl. Instrum. Methods Phys. Res., Sect. A* **506**, 250 (2003).
- [35] J. Allison *et al.* (Geant4 Collaboration), Geant4 developments and applications, *IEEE Trans. Nucl. Sci.* **53**, 270 (2006).
- [36] T. Skwarnicki, A study of the radiative cascade transitions between the Upsilon-prime and Upsilon resonances, Ph.D. thesis, Institute of Nuclear Physics, Krakow, 1986; Report No. DESY-F31-86-02.
- [37] K. S. Cranmer, Kernel estimation in high-energy physics, *Comput. Phys. Commun.* **136**, 198 (2001).
- [38] M. Pivk and F. R. Le Diberder, sPlot: A statistical tool to unfold data distributions, *Nucl. Instrum. Methods Phys. Res., Sect. A* **555**, 356 (2005).
- [39] V. Gligorov, C. Thomas, and M. Williams, The HLT inclusive B triggers, Report No. LHCb-PUB-2011-016.
- [40] R. Aaij *et al.* (LHCb Collaboration), Measurement of relative branching fractions of B decays to $\psi(2S)$ and J/ψ mesons, *Eur. Phys. J. C* **72**, 2118 (2012).

R. Aaij,³⁸ B. Adeva,³⁷ M. Adinolfi,⁴⁶ A. Affolder,⁵² Z. Ajaltouni,⁵ S. Akar,⁶ J. Albrecht,⁹ F. Alessio,³⁸ M. Alexander,⁵¹ S. Ali,⁴¹ G. Alkhazov,³⁰ P. Alvarez Cartelle,⁵³ A. A. Alves Jr,⁵⁷ S. Amato,² S. Amerio,²² Y. Amhis,⁷ L. An,³ J. Anderson,⁴⁰ G. Andreassi,³⁹ M. Andreotti,^{16,g} J. E. Andrews,⁵⁸ R. B. Appleby,⁵⁴ O. Aquines Gutierrez,¹⁰ F. Archilli,³⁸ P. d'Argent,¹¹ A. Artamonov,³⁵ M. Artuso,⁵⁹ E. Aslanides,⁶ G. Auriemma,^{25,n} M. Baalouch,⁵ S. Bachmann,¹¹ J. J. Back,⁴⁸ A. Badalov,³⁶ C. Baesso,⁶⁰ W. Baldini,^{16,38} R. J. Barlow,⁵⁴ C. Barschel,³⁸ S. Barsuk,⁷ W. Barter,³⁸ V. Batozskaya,²⁸ V. Battista,³⁹ A. Bay,³⁹ L. Beaucourt,⁴ J. Beddow,⁵¹ F. Bedeschi,²³ I. Bediaga,¹ L. J. Bel,⁴¹ V. Bellee,³⁹ I. Belyaev,³¹ E. Ben-Haim,⁸ G. Bencivenni,¹⁸ S. Benson,³⁸ J. Benton,⁴⁶ A. Berezhnoy,³² R. Bernet,⁴⁰ A. Bertolin,²² M.-O. Bettler,³⁸ M. van Beuzekom,⁴¹ A. Bien,¹¹ S. Bifani,⁴⁵ T. Bird,⁵⁴ A. Birnkraut,⁹ A. Bizzeti,^{17,i} T. Blake,⁴⁸ F. Blanc,³⁹ J. Blouw,¹⁰ S. Blusk,⁵⁹ V. Bocci,²⁵ A. Bondar,³⁴ N. Bondar,^{30,38} W. Bonivento,¹⁵ S. Borghi,⁵⁴ M. Borsato,⁷ T. J. V. Bowcock,⁵² E. Bowen,⁴⁰ C. Bozzi,¹⁶ S. Braun,¹¹ D. Brett,⁵⁴ M. Britsch,¹⁰ T. Britton,⁵⁹ J. Brodzicka,⁵⁴ N. H. Brook,⁴⁶ A. Bursche,⁴⁰ J. Buytaert,³⁸ S. Cadeddu,¹⁵ R. Calabrese,^{16,g} M. Calvi,^{20,k} M. Calvo Gomez,^{36,p} P. Campana,¹⁸ D. Campora Perez,³⁸ L. Capriotti,⁵⁴ A. Carbone,^{14,e} G. Carboni,^{24,l} R. Cardinale,^{19,j} A. Cardini,¹⁵ P. Carniti,²⁰ L. Carson,⁵⁰ K. Carvalho Akiba,^{2,38} G. Casse,⁵² L. Cassina,^{20,k} L. Castillo Garcia,³⁸ M. Cattaneo,³⁸ Ch. Cauet,⁹ G. Cavallero,¹⁹ R. Cenci,^{23,t} M. Charles,⁸ Ph. Charpentier,³⁸ M. Chefdeville,⁴ S. Chen,⁵⁴ S.-F. Cheung,⁵⁵ N. Chiapolini,⁴⁰ M. Chrzaszcz,⁴⁰ X. Cid Vidal,³⁸ G. Ciezarek,⁴¹ P. E. L. Clarke,⁵⁰ M. Clemencic,³⁸ H. V. Cliff,⁴⁷ J. Closier,³⁸ V. Coco,³⁸ J. Cogan,⁶ E. Cogneras,⁵ V. Cogoni,^{15,f} L. Cojocariu,²⁹ G. Collazuol,²² P. Collins,³⁸ A. Comerma-Montells,¹¹ A. Contu,^{15,38} A. Cook,⁴⁶ M. Coombes,⁴⁶ S. Coquereau,⁸ G. Corti,³⁸ M. Corvo,^{16,g} B. Couturier,³⁸ G. A. Cowan,⁵⁰ D. C. Craik,⁴⁸ A. Crocombe,⁴⁸ M. Cruz Torres,⁶⁰ S. Cunliffe,⁵³ R. Currie,⁵³ C. D'Ambrosio,³⁸ E. Dall'Occo,⁴¹ J. Dalseno,⁴⁶ P. N. Y. David,⁴¹ A. Davis,⁵⁷ K. De Bruyn,⁴¹ S. De Capua,⁵⁴ M. De Cian,¹¹ J. M. De Miranda,¹ L. De Paula,² P. De Simone,¹⁸ C.-T. Dean,⁵¹ D. Decamp,⁴ M. Deckenhoff,⁹

- L. Del Buono,⁸ N. Déléage,⁴ M. Demmer,⁹ D. Derkach,⁵⁵ O. Deschamps,⁵ F. Dettori,³⁸ B. Dey,²¹ A. Di Canto,³⁸ F. Di Ruscio,²⁴ H. Dijkstra,³⁸ S. Donleavy,⁵² F. Dordei,¹¹ M. Dorigo,³⁹ A. Dosil Suárez,³⁷ D. Dossett,⁴⁸ A. Dovbnya,⁴³ K. Dreimanis,⁵² L. Dufour,⁴¹ G. Dujany,⁵⁴ F. Dupertuis,³⁹ P. Durante,³⁸ R. Dzhelyadin,³⁵ A. Dziurda,²⁶ A. Dzyuba,³⁰ S. Easo,^{49,38} U. Egede,⁵³ V. Egorychev,³¹ S. Eidelman,³⁴ S. Eisenhardt,⁵⁰ U. Eitschberger,⁹ R. Ekelhof,⁹ L. Eklund,⁵¹ I. El Rifai,⁵ Ch. Elsasser,⁴⁰ S. Ely,⁵⁹ S. Esen,¹¹ H. M. Evans,⁴⁷ T. Evans,⁵⁵ A. Falabella,¹⁴ C. Färber,³⁸ C. Farinelli,⁴¹ N. Farley,⁴⁵ S. Farry,⁵² R. Fay,⁵² D. Ferguson,⁵⁰ V. Fernandez Albor,³⁷ F. Ferrari,¹⁴ F. Ferreira Rodrigues,¹ M. Ferro-Luzzi,³⁸ S. Filippov,³³ M. Fiore,^{16,38,g} M. Fiorini,^{16,g} M. Firlej,²⁷ C. Fitzpatrick,³⁹ T. Fiutowski,²⁷ K. Fohl,³⁸ P. Fol,⁵³ M. Fontana,¹⁰ F. Fontanelli,^{19,j} R. Forty,³⁸ O. Francisco,² M. Frank,³⁸ C. Frei,³⁸ M. Frosini,¹⁷ J. Fu,²¹ E. Furfaro,^{24,l} A. Gallas Torreira,³⁷ D. Galli,^{14,e} S. Gallorini,^{22,38} S. Gambetta,⁵⁰ M. Gandelman,² P. Gandini,⁵⁵ Y. Gao,³ J. García Pardiñas,³⁷ J. Garra Tico,⁴⁷ L. Garrido,³⁶ D. Gascon,³⁶ C. Gaspar,³⁸ R. Gauld,⁵⁵ L. Gavardi,⁹ G. Gazzoni,⁵ A. Geraci,^{21,v} D. Gerick,¹¹ E. Gersabeck,¹¹ M. Gersabeck,⁵⁴ T. Gershon,⁴⁸ Ph. Ghez,⁴ A. Gianelle,²² S. Giani,³⁹ V. Gibson,⁴⁷ O. G. Girard,³⁹ L. Giubega,²⁹ V. V. Gligorov,³⁸ C. Göbel,⁶⁰ D. Golubkov,³¹ A. Golutvin,^{53,31,38} A. Gomes,^{1,b} C. Gotti,^{20,k} M. Grabalosa Gándara,⁵ R. Graciani Diaz,³⁶ L. A. Granado Cardoso,³⁸ E. Graugés,³⁶ E. Graverini,⁴⁰ G. Graziani,¹⁷ A. Grecu,²⁹ E. Greening,⁵⁵ S. Gregson,⁴⁷ P. Griffith,⁴⁵ L. Grillo,¹¹ O. Grünberg,⁶³ B. Gui,⁵⁹ E. Gushchin,³³ Yu. Guz,^{35,38} T. Gys,³⁸ T. Hadavizadeh,⁵⁵ C. Hadjivasilou,⁵⁹ G. Haefeli,³⁹ C. Haen,³⁸ S. C. Haines,⁴⁷ S. Hall,⁵³ B. Hamilton,⁵⁸ X. Han,¹¹ S. Hansmann-Menzemer,¹¹ N. Harnew,⁵⁵ J. Harrison,⁵⁴ J. He,³⁸ T. Head,³⁹ V. Heijne,⁴¹ K. Hennessy,⁵² P. Henrard,⁵ L. Henry,⁸ J. A. Hernando Morata,³⁷ E. van Herwijnen,³⁸ M. Heß,⁶³ A. Hicheur,² D. Hill,⁵⁵ M. Hoballah,⁵ C. Hombach,⁵⁴ W. Hulsbergen,⁴¹ T. Humair,⁵³ N. Hussain,⁵⁵ D. Hutchcroft,⁵² D. Hynds,⁵¹ M. Idzik,²⁷ P. Ilten,⁵⁶ R. Jacobsson,³⁸ A. Jaeger,¹¹ J. Jalocha,⁵⁵ E. Jans,⁴¹ A. Jawahery,⁵⁸ F. Jing,³ M. John,⁵⁵ D. Johnson,³⁸ C. R. Jones,⁴⁷ C. Joram,³⁸ B. Jost,³⁸ N. Jurik,⁵⁹ S. Kandybei,⁴³ W. Kanso,⁶ M. Karacson,³⁸ T. M. Karbach,^{38,a} S. Karodia,⁵¹ M. Kelsey,⁵⁹ I. R. Kenyon,⁴⁵ M. Kenzie,³⁸ T. Ketel,⁴² B. Khanji,^{20,38,k} C. Khurewathanakul,³⁹ S. Klaver,⁵⁴ K. Klimaszewski,²⁸ O. Kochebina,⁷ M. Kolpin,¹¹ I. Komarov,³⁹ R. F. Koopman,⁴² P. Koppenburg,^{41,38} M. Kozeiha,⁵ L. Kravchuk,³³ K. Kreplin,¹¹ M. Kreps,⁴⁸ G. Krocker,¹¹ P. Krokovny,³⁴ F. Kruse,⁹ W. Kucewicz,^{26,o} M. Kucharczyk,²⁶ V. Kudryavtsev,³⁴ A. K. Kuonen,³⁹ K. Kurek,²⁸ T. Kvaratskheliya,³¹ D. Lacarrere,³⁸ G. Lafferty,⁵⁴ A. Lai,¹⁵ D. Lambert,⁵⁰ G. Lanfranchi,¹⁸ C. Langenbruch,⁴⁸ B. Langhans,³⁸ T. Latham,⁴⁸ C. Lazzeroni,⁴⁵ R. Le Gac,⁶ J. van Leerdam,⁴¹ J.-P. Lees,⁴ R. Lefèvre,⁵ A. Leflat,^{32,38} J. Lefrançois,⁷ O. Leroy,⁶ T. Lesiak,²⁶ B. Leverington,¹¹ Y. Li,⁷ T. Likhomanenko,^{65,64} M. Liles,⁵² R. Lindner,³⁸ C. Linn,³⁸ F. Lionetto,⁴⁰ B. Liu,¹⁵ X. Liu,³ D. Loh,⁴⁸ S. Lohn,³⁸ I. Longstaff,⁵¹ J. H. Lopes,² D. Lucchesi,^{22,r} M. Lucio Martinez,³⁷ H. Luo,⁵⁰ A. Lupato,²² E. Luppi,^{16,g} O. Lupton,⁵⁵ N. Lusardi,²¹ A. Lusiani,²³ F. Machefert,⁷ F. Maciuc,²⁹ O. Maev,³⁰ K. Maguire,⁵⁴ S. Malde,⁵⁵ A. Malinin,⁶⁴ G. Manca,⁷ G. Mancinelli,⁶ P. Manning,⁵⁹ A. Mapelli,³⁸ J. Maratas,⁵ J. F. Marchand,⁴ U. Marconi,¹⁴ C. Marin Benito,³⁶ P. Marino,^{23,38,t} R. Märki,³⁹ J. Marks,¹¹ G. Martellotti,²⁵ M. Martin,⁶ M. Martinelli,³⁹ D. Martinez Santos,³⁷ F. Martinez Vidal,⁶⁶ D. Martins Tostes,² A. Massafferri,¹ R. Matev,³⁸ A. Mathad,⁴⁸ Z. Mathe,³⁸ C. Matteuzzi,²⁰ K. Matthieu,¹¹ A. Mauri,⁴⁰ B. Maurin,³⁹ A. Mazurov,⁴⁵ M. McCann,⁵³ J. McCarthy,⁴⁵ A. McNab,⁵⁴ R. McNulty,¹² B. Meadows,⁵⁷ F. Meier,⁹ M. Meissner,¹¹ D. Melnychuk,²⁸ M. Merk,⁴¹ D. A. Milanes,⁶² M.-N. Minard,⁴ D. S. Mitzel,¹¹ J. Molina Rodriguez,⁶⁰ I. A. Monroy,⁶² S. Monteil,⁵ M. Morandin,²² P. Morawski,²⁷ A. Mordà,⁶ M. J. Morello,^{23,t} J. Moron,²⁷ A. B. Morris,⁵⁰ R. Mountain,⁵⁹ F. Muheim,⁵⁰ J. Müller,⁹ K. Müller,⁴⁰ V. Müller,⁹ M. Mussini,¹⁴ B. Muster,³⁹ P. Naik,⁴⁶ T. Nakada,³⁹ R. Nandakumar,⁴⁹ A. Nandi,⁵⁵ I. Nasteva,² M. Needham,⁵⁰ N. Neri,²¹ S. Neubert,¹¹ N. Neufeld,³⁸ M. Neuner,¹¹ A. D. Nguyen,³⁹ T. D. Nguyen,³⁹ C. Nguyen-Mau,^{39,q} V. Niess,⁵ R. Niet,⁹ N. Nikitin,³² T. Nikodem,¹¹ D. Ninci,²³ A. Novoselov,³⁵ D. P. O'Hanlon,⁴⁸ A. Oblakowska-Mucha,²⁷ V. Obraztsov,³⁵ S. Ogilvy,⁵¹ O. Okhrimenko,⁴⁴ R. Oldeman,^{15,f} C. J. G. Onderwater,⁶⁷ B. Osorio Rodrigues,¹ J. M. Otalora Goicochea,² A. Otto,³⁸ P. Owen,⁵³ A. Oyanguren,⁶⁶ A. Palano,^{13,d} F. Palombo,^{21,u} M. Palutan,¹⁸ J. Panman,³⁸ A. Papanestis,⁴⁹ M. Pappagallo,⁵¹ L. L. Pappalardo,^{16,g} C. Pappenheimer,⁵⁷ C. Parkes,⁵⁴ G. Passaleva,¹⁷ G. D. Patel,⁵² M. Patel,⁵³ C. Patrignani,^{19,j} A. Pearce,^{54,49} A. Pellegrino,⁴¹ G. Penso,^{25,m} M. Pepe Altarelli,³⁸ S. Perazzini,^{14,e} P. Perret,⁵ L. Pescatore,⁴⁵ K. Petridis,⁴⁶ A. Petrolini,^{19,j} M. Petruzzo,²¹ E. Picatoste Olloqui,³⁶ B. Pietrzyk,⁴ T. Pilat,⁴⁸ D. Pinci,²⁵ A. Pistone,¹⁹ A. Piucci,¹¹ S. Playfer,⁵⁰ M. Plo Casasus,³⁷ T. Poikela,³⁸ F. Polci,⁸ A. Poluektov,^{48,34} I. Polyakov,³¹ E. Polycarpo,² A. Popov,³⁵ D. Popov,^{10,38} B. Popovici,²⁹ C. Potterat,² E. Price,⁴⁶ J. D. Price,⁵² J. Prisciandaro,³⁹ A. Pritchard,⁵² C. Prouve,⁴⁶ V. Pugatch,⁴⁴ A. Puig Navarro,³⁹ G. Punzi,^{23,s} W. Qian,⁴ R. Quagliani,^{7,46} B. Rachwal,²⁶ J. H. Rademacker,⁴⁶ M. Rama,²³ M. S. Rangel,² I. Raniuk,⁴³ N. Rauschmayr,³⁸ G. Raven,⁴² F. Redi,⁵³ S. Reichert,⁵⁴ M. M. Reid,⁴⁸ A. C. dos Reis,¹ S. Ricciardi,⁴⁹ S. Richards,⁴⁶ M. Rihl,³⁸ K. Rinnert,⁵² V. Rives Molina,³⁶ P. Robbe,^{7,38} A. B. Rodrigues,¹ E. Rodrigues,⁵⁴ J. A. Rodriguez Lopez,⁶² P. Rodriguez Perez,⁵⁴ S. Roiser,³⁸ V. Romanovsky,³⁵ A. Romero Vidal,³⁷ J. W. Ronayne,¹²

M. Rotondo,²² J. Rouvinet,³⁹ T. Ruf,³⁸ H. Ruiz,³⁶ P. Ruiz Valls,⁶⁶ J. J. Saborido Silva,³⁷ N. Sagidova,³⁰ P. Sail,⁵¹ B. Saitta,^{15,f} V. Salustino Guimaraes,² C. Sanchez Mayordomo,⁶⁶ B. Sanmartin Sedes,³⁷ R. Santacesaria,²⁵ C. Santamarina Rios,³⁷ M. Santimaria,¹⁸ E. Santovetti,^{24,l} A. Sarti,^{18,m} C. Satriano,^{25,n} A. Satta,²⁴ D. M. Saunders,⁴⁶ D. Savrina,^{31,32} M. Schiller,³⁸ H. Schindler,³⁸ M. Schlupp,⁹ M. Schmelling,¹⁰ T. Schmelzer,⁹ B. Schmidt,³⁸ O. Schneider,³⁹ A. Schopper,³⁸ M. Schubiger,³⁹ M.-H. Schune,⁷ R. Schwemmer,³⁸ B. Sciascia,¹⁸ A. Sciubba,^{25,m} A. Semennikov,³¹ N. Serra,⁴⁰ J. Serrano,⁶ L. Sestini,²² P. Seyfert,²⁰ M. Shapkin,³⁵ I. Shapoval,^{16,43,g} Y. Shcheglov,³⁰ T. Shears,⁵² L. Shekhtman,³⁴ V. Shevchenko,⁶⁴ A. Shires,⁹ B. G. Siddi,¹⁶ R. Silva Coutinho,⁴⁸ G. Simi,²² M. Sirendi,⁴⁷ N. Skidmore,⁴⁶ I. Skillicorn,⁵¹ T. Skwarnicki,⁵⁹ E. Smith,^{55,49} E. Smith,⁵³ I. T. Smith,⁵⁰ J. Smith,⁴⁷ M. Smith,⁵⁴ H. Snoek,⁴¹ M. D. Sokoloff,^{57,38} F. J. P. Soler,⁵¹ F. Soomro,³⁹ D. Souza,⁴⁶ B. Souza De Paula,² B. Spaan,⁹ P. Spradlin,⁵¹ S. Sridharan,³⁸ F. Stagni,³⁸ M. Stahl,¹¹ S. Stahl,³⁸ O. Steinkamp,⁴⁰ O. Stenyakin,³⁵ F. Sterpka,⁵⁹ S. Stevenson,⁵⁵ S. Stoica,²⁹ S. Stone,⁵⁹ B. Storaci,⁴⁰ S. Stracka,^{23,t} M. Stratciuc,²⁹ U. Straumann,⁴⁰ L. Sun,⁵⁷ W. Sutcliffe,⁵³ K. Swientek,²⁷ S. Swientek,⁹ V. Syropoulos,⁴² M. Szczekowski,²⁸ P. Szczypka,^{39,38} T. Szumlak,²⁷ S. T'Jampens,⁴ A. Tayduganov,⁶ T. Tekampe,⁹ M. Teklichyn,⁷ G. Tellarini,^{16,g} F. Teubert,³⁸ C. Thomas,⁵⁵ E. Thomas,³⁸ J. van Tilburg,⁴¹ V. Tisserand,⁴ M. Tobin,³⁹ J. Todd,⁵⁷ S. Tolk,⁴² L. Tomassetti,^{16,g} D. Tonelli,³⁸ S. Topp-Joergensen,⁵⁵ N. Torr,⁵⁵ E. Tournefier,⁴ S. Tourneur,³⁹ K. Trabelsi,³⁹ M. T. Tran,³⁹ M. Tresch,⁴⁰ A. Trisovic,³⁸ A. Tsaregorodtsev,⁶ P. Tsopelas,⁴¹ N. Tuning,^{41,38} A. Ukleja,²⁸ A. Ustyuzhanin,^{65,64} U. Uwer,¹¹ C. Vacca,^{15,f} V. Vagnoni,¹⁴ G. Valenti,¹⁴ A. Vallier,⁷ R. Vazquez Gomez,¹⁸ P. Vazquez Regueiro,³⁷ C. Vázquez Sierra,³⁷ S. Vecchi,¹⁶ J. J. Velthuis,⁴⁶ M. Veltri,^{17,h} G. Veneziano,³⁹ M. Vesterinen,¹¹ B. Viaud,⁷ D. Vieira,² M. Vieites Diaz,³⁷ X. Vilasis-Cardona,^{36,p} A. Vollhardt,⁴⁰ D. Volyanskyy,¹⁰ D. Voong,⁴⁶ A. Vorobyev,³⁰ V. Vorobyev,³⁴ C. Voß,⁶³ J. A. de Vries,⁴¹ R. Waldi,⁶³ C. Wallace,⁴⁸ R. Wallace,¹² J. Walsh,²³ S. Wandernoth,¹¹ J. Wang,⁵⁹ D. R. Ward,⁴⁷ N. K. Watson,⁴⁵ D. Websdale,⁵³ A. Weiden,⁴⁰ M. Whitehead,⁴⁸ G. Wilkinson,^{55,38} M. Wilkinson,⁵⁹ M. Williams,³⁸ M. P. Williams,⁴⁵ M. Williams,⁵⁶ T. Williams,⁴⁵ F. F. Wilson,⁴⁹ J. Wimberley,⁵⁸ J. Wishahi,⁹ W. Wislicki,²⁸ M. Witek,²⁶ G. Wormser,⁷ S. A. Wotton,⁴⁷ S. Wright,⁴⁷ K. Wyllie,³⁸ Y. Xie,⁶¹ Z. Xu,³⁹ Z. Yang,³ J. Yu,⁶¹ X. Yuan,³⁴ O. Yushchenko,³⁵ M. Zangoli,¹⁴ M. Zavertyaev,^{10,c} L. Zhang,³ Y. Zhang,³ A. Zhelezov,¹¹ A. Zhokhov,³¹ L. Zhong³ and S. Zucchelli¹⁴

(LHCb collaboration)

¹*Centro Brasileiro de Pesquisas Físicas (CBPF), Rio de Janeiro, Brazil*²*Universidade Federal do Rio de Janeiro (UFRJ), Rio de Janeiro, Brazil*³*Center for High Energy Physics, Tsinghua University, Beijing, China*⁴*LAPP, Université Savoie Mont-Blanc, CNRS/IN2P3, Annecy-Le-Vieux, France*⁵*Clermont Université, Université Blaise Pascal, CNRS/IN2P3, LPC, Clermont-Ferrand, France*⁶*CPPM, Aix-Marseille Université, CNRS/IN2P3, Marseille, France*⁷*LAL, Université Paris-Sud, CNRS/IN2P3, Orsay, France*⁸*LPNHE, Université Pierre et Marie Curie, Université Paris Diderot, CNRS/IN2P3, Paris, France*⁹*Fakultät Physik, Technische Universität Dortmund, Dortmund, Germany*¹⁰*Max-Planck-Institut für Kernphysik (MPIK), Heidelberg, Germany*¹¹*Physikalisch Institut, Ruprecht-Karls-Universität Heidelberg, Heidelberg, Germany*¹²*School of Physics, University College Dublin, Dublin, Ireland*¹³*Sezione INFN di Bari, Bari, Italy*¹⁴*Sezione INFN di Bologna, Bologna, Italy*¹⁵*Sezione INFN di Cagliari, Cagliari, Italy*¹⁶*Sezione INFN di Ferrara, Ferrara, Italy*¹⁷*Sezione INFN di Firenze, Firenze, Italy*¹⁸*Laboratori Nazionali dell'INFN di Frascati, Frascati, Italy*¹⁹*Sezione INFN di Genova, Genova, Italy*²⁰*Sezione INFN di Milano Bicocca, Milano, Italy*²¹*Sezione INFN di Milano, Milano, Italy*²²*Sezione INFN di Padova, Padova, Italy*²³*Sezione INFN di Pisa, Pisa, Italy*²⁴*Sezione INFN di Roma Tor Vergata, Roma, Italy*²⁵*Sezione INFN di Roma La Sapienza, Roma, Italy*²⁶*Henryk Niewodniczanski Institute of Nuclear Physics Polish Academy of Sciences, Kraków, Poland*²⁷*AGH - University of Science and Technology, Faculty of Physics and Applied Computer Science, Kraków, Poland*²⁸*National Center for Nuclear Research (NCBJ), Warsaw, Poland*

- ²⁹Horia Hulubei National Institute of Physics and Nuclear Engineering, Bucharest-Magurele, Romania
³⁰Petersburg Nuclear Physics Institute (PNPI), Gatchina, Russia
³¹Institute of Theoretical and Experimental Physics (ITEP), Moscow, Russia
³²Institute of Nuclear Physics, Moscow State University (SINP MSU), Moscow, Russia
³³Institute for Nuclear Research of the Russian Academy of Sciences (INR RAN), Moscow, Russia
³⁴Budker Institute of Nuclear Physics (SB RAS) and Novosibirsk State University, Novosibirsk, Russia
³⁵Institute for High Energy Physics (IHEP), Protvino, Russia
³⁶Universitat de Barcelona, Barcelona, Spain
³⁷Universidad de Santiago de Compostela, Santiago de Compostela, Spain
³⁸European Organization for Nuclear Research (CERN), Geneva, Switzerland
³⁹Ecole Polytechnique Fédérale de Lausanne (EPFL), Lausanne, Switzerland
⁴⁰Physik-Institut, Universität Zürich, Zürich, Switzerland
⁴¹Nikhef National Institute for Subatomic Physics, Amsterdam, The Netherlands
⁴²Nikhef National Institute for Subatomic Physics and VU University Amsterdam, Amsterdam, The Netherlands
⁴³NSC Kharkiv Institute of Physics and Technology (NSC KIPT), Kharkiv, Ukraine
⁴⁴Institute for Nuclear Research of the National Academy of Sciences (KINR), Kyiv, Ukraine
⁴⁵University of Birmingham, Birmingham, United Kingdom
⁴⁶H.H. Wills Physics Laboratory, University of Bristol, Bristol, United Kingdom
⁴⁷Cavendish Laboratory, University of Cambridge, Cambridge, United Kingdom
⁴⁸Department of Physics, University of Warwick, Coventry, United Kingdom
⁴⁹STFC Rutherford Appleton Laboratory, Didcot, United Kingdom
⁵⁰School of Physics and Astronomy, University of Edinburgh, Edinburgh, United Kingdom
⁵¹School of Physics and Astronomy, University of Glasgow, Glasgow, United Kingdom
⁵²Oliver Lodge Laboratory, University of Liverpool, Liverpool, United Kingdom
⁵³Imperial College London, London, United Kingdom
⁵⁴School of Physics and Astronomy, University of Manchester, Manchester, United Kingdom
⁵⁵Department of Physics, University of Oxford, Oxford, United Kingdom
⁵⁶Massachusetts Institute of Technology, Cambridge 02139, Massachusetts, USA
⁵⁷University of Cincinnati, Cincinnati 45221, Ohio, USA
⁵⁸University of Maryland, College Park, Maryland 20742, USA
⁵⁹Syracuse University, Syracuse 13244, New York, USA
⁶⁰Pontifícia Universidade Católica do Rio de Janeiro (PUC-Rio), Rio de Janeiro, Brazil, (associated with Universidade Federal do Rio de Janeiro (UFRJ), Rio de Janeiro, Brazil)
⁶¹Institute of Particle Physics, Central China Normal University, Wuhan, Hubei, China, (associated with Center for High Energy Physics, Tsinghua University, Beijing, China)
⁶²Departamento de Física, Universidad Nacional de Colombia, Bogota, Colombia, (associated with LPNHE, Université Pierre et Marie Curie, Université Paris Diderot, CNRS/IN2P3, Paris, France)
⁶³Institut für Physik, Universität Rostock, Rostock, Germany, (associated with Physikalisches Institut, Ruprecht-Karls-Universität Heidelberg, Heidelberg, Germany)
⁶⁴National Research Centre Kurchatov Institute, Moscow, Russia, (associated with Institute of Theoretical and Experimental Physics (ITEP), Moscow, Russia)
⁶⁵Yandex School of Data Analysis, Moscow, Russia, (associated with Institute of Theoretical and Experimental Physics (ITEP), Moscow, Russia)
⁶⁶Instituto de Física Corpuscular (IFIC), Universitat de València-CSIC, Valencia, Spain, (associated with Universitat de Barcelona, Barcelona, Spain)
⁶⁷Van Swinderen Institute, University of Groningen, Groningen, The Netherlands, (associated with Nikhef National Institute for Subatomic Physics, Amsterdam, The Netherlands)

^aDeceased.^bAlso at Universidade Federal do Triângulo Mineiro (UFTM), Uberaba-MG, Brazil.^cAlso at P.N. Lebedev Physical Institute, Russian Academy of Science (LPI RAS), Moscow, Russia.^dAlso at Università di Bari, Bari, Italy.^eAlso at Università di Bologna, Bologna, Italy.^fAlso at Università di Cagliari, Cagliari, Italy.^gAlso at Università di Ferrara, Ferrara, Italy.^hAlso at Università di Urbino, Urbino, Italy.ⁱAlso at Università di Modena e Reggio Emilia, Modena, Italy.^jAlso at Università di Genova, Genova, Italy.^kAlso at Università di Milano Bicocca, Milano, Italy.

¹Also at Università di Roma Tor Vergata, Roma, Italy.

^mAlso at Università di Roma La Sapienza, Roma, Italy.

ⁿAlso at Università della Basilicata, Potenza, Italy

^oAlso at AGH - University of Science and Technology, Faculty of Computer Science, Electronics and Telecommunications, Kraków, Poland.

^pAlso at LIFAELS, La Salle, Universitat Ramon Llull, Barcelona, Spain.

^qAlso at Hanoi University of Science, Hanoi, Viet Nam.

^rAlso at Università di Padova, Padova, Italy.

^sAlso at Università di Pisa, Pisa, Italy.

^tAlso at Scuola Normale Superiore, Pisa, Italy.

^uAlso at Università degli Studi di Milano, Milano, Italy.

^vAlso at Politecnico di Milano, Milano, Italy.